Topology, Geometry and Mechanics of Z-plasty

Elisabetta A. Matsumoto[1], Haiyi Liang[2], L. Mahadevan[1,3]
[1] *Paulson School of Engineering and Applied Sciences, Wyss Institute for Biologically Inspired Engineering,*
[2] *CAS Key Laboratory of Mechanical Behavior and Design of Materials, University of Science and Technology of China, Hefei, China,*
[3] *Departments of Physics and Organismic and Evolutionary Biology, and Kavli Institute for NanoBio Science and Technology, Harvard University, 29 Oxford Street, Cambridge, MA 02138*
(Dated: May 1, 2016)

Reconstructive surgery frequently requires the topological manipulation of the skin to minimize post-operative scarring. One of the most common surgical techniques for this is termed Z-plasty and involves the creation of a Z-shaped cut from a simple linear cut along with a rotational transposition of two triangular pedicle flaps before restitching the wound. This leads to a local reorientation of the anisotropic stress field, thus reducing the potential for scarring. We complement this topological description of Z-plasty by analyzing the geometry and mechanics of the cutting and restitching process, which forms a disclination quadrupole. By varying the angle in the Z-plasty, we explore the consequence on the stress on the wound. A set of simple physical Z-plasty experiments with foam sheets confirms our findings. Our study rationalizes surgical choices of this angle, and by characterizing the stresses along the cut, may allow for surgical decisions.

Scar formation is a natural part of the wound healing process, in which fibroblasts migrate throughout the wound and produce collagen [1]. The pathophysiology of wound healing involves a series of processes including fibroblast proliferation and apoptosis, extracellular matrix (ECM) synthesis, remodeling, and degradation. Complementing the active roles of cytokines, growth factors and hormones, the mechanical response of skin is an important factor in regulating scar formation and evolution. Experiments suggest that suppressed cellular apoptosis from mechanical tension leads to hypertrophic scaring [2]. Likewise, collagen bundles in the dermis align with the wound to counteract stretching from the neighboring ECM, resulting in stiffening of scar tissue [2–5]. Often the change in elastic modulus between healthy skin and scar tissue results in deformations of the surrounding healthy tissue [6]. In severe cases, hypertrophic scaring develops as skin fibrosis after surgical or traumatic injuries, resulting in æsthetic defects, body disfigurement or organ dysfunction. Thus surgical intervention is required to restore function and æsthetics. A particularly common class of plastic surgeries that do this are variants of what is commonly known as Z-plasty, first introduced in 1837 to correct the coarctation of the eyelid [7, 8]. It involves a topological transformation of a "Z"-shaped incision that exposes two triangular flaps. When these flaps are transposed and stitched together, the original linear cut (the central limb of the Z) rotates, reducing the opening stress on the wound. Frequently employed for the prevention or revision of scarification of linear wounds, reorienting scars parallel to the local directions of maximal tension in the skin [9] minimizes fibrosis, thus enhancing flexibility. Also used in scar revision to relieve skin contracture due to burns or other trauma, this surgery elongates a localized region of tissue, thus restoring mobility to joints or other highly curved parts of the body, such as the face. In this Letter, we present an elastic model for Z-plasty with the aim of understanding both the geometry and stresses in the final structure introduced by this topological transformation. This allows us to propose a simple design rule for the angles of the additional incisions that the surgeon has freedom to choose.

In a Z-plasty, a primary wound of length ℓ (chosen here to be oriented along the direction of smaller principal stress $\mathbf{e_y}$), depicted as AB in Fig. 1a, is made seemingly worse by introducing two auxiliary incisions at either end of the wound, AC and BD, at an angle α to the wound [10]. This Z-shaped incision outlines two similar triangular flaps, BCA and ADB, whose shared middle limb corresponds to the primary incision (see Fig. 1a). Next, the two flaps are excised from the underlying tissues, transposed to yield a new topological configuration (Fig. 1b). The resulting "S"-shaped structure has a middle branch created by joining two flaps along their auxiliary incisions; when this structure is allowed to reach elastic equilibrium, the flaps rotate by an amount θ (Fig. 1a) while central limb of the Z, which corresponds to the original wound, rotates by an amount ϕ (Fig. 1c). Both these angles are functions of the cutting α and the ambient stress field. This geometrical transformation is accompanied by a transverse lengthening strain ε_h and a lateral shortening strain ε_w. To understand this in a simple setting, we mimic the basic z-plasty surgery on a sheet of foam-rubber, as shown in Fig.1c), and see that a reference mesh in the vicinity of the "wound" is strongly distorted locally, but remains relatively undistorted in the far field.

Surgeons typically estimate the final shape of

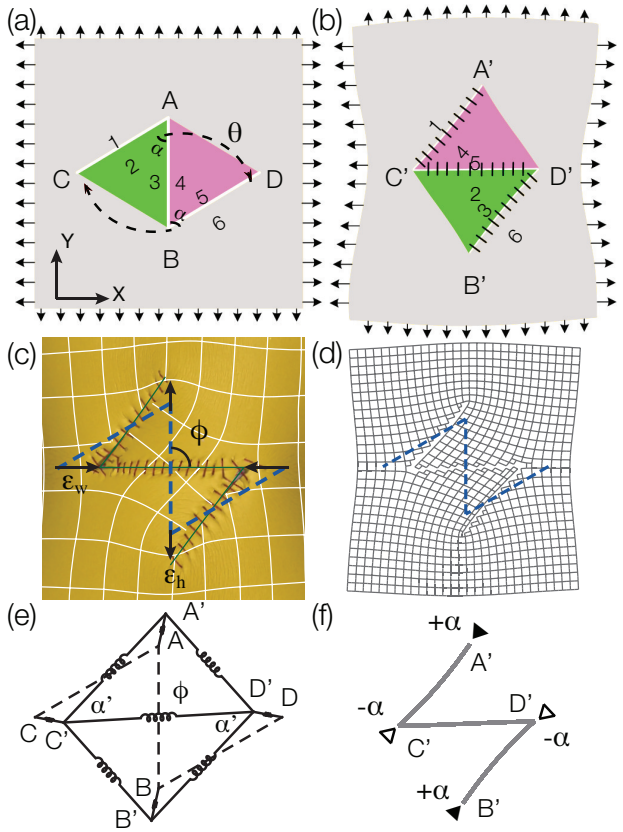

FIG. 1. (a) The cuts that characterize the Z-plasty; AB is the original cut while the new cuts AC and BD make an angle α with the original one and have a length ℓ. (b) The topological reconnection. The sides that are originally paired, i.e. 1-2, 3-4, 5-6 are rotated and stitched together as 1-4, 2-5 and 3-6 after surgery. This causes the flaps to rotate by an amount θ and the limbs to rotate by an amount ϕ. (c) A z-plasty in a foam-rubber sheet shows the strong distortion of the mesh locally. This geometric transformation is accompanied by a lateral shrinkage strain ε_w and a transverse extension strain ε_h. (d) Numerical simulations of an elastic sheet subject to Z-plasty show a distorted mesh around a Z-plasty. (The dashed lines outline the initial incision.) (e) A simple model of the change in network topology based on a few springs captures the essence of the transformation. (f) A Z-plasty is topologically a disclination quadrupole made of two positive disclinations of strength α that lead to local stretching and shear and two negative disclinations of strength $-\alpha$ that lead to local compression and shear.

a Z-plasty by ignoring any contributions from elastic deformation and assuming rigid rotation of the parallelogram flaps so that the long diagonal is aligned along $\mathbf{e}_y$ after the transposal [11–13]. Geometry alone dictates that the rigid rotation of the left flap from ΔCAB to $\Delta C'D'B'$ is $\theta^g = \sin^{-1}(\sin\alpha/\sqrt{5-4\cos\alpha})$, where the superscript g denotes surgeon's geometric estimate. The rotation of the central limb counterclockwise with respect to the $+\mathbf{e}_y$ direction is $\phi^g = \cos^{-1}(\vec{A}\cdot\vec{D}'/(|A||D'|)) = \cos^{-1}((1-2\cos\alpha)/\sqrt{5-4\cos\alpha}) = 180-\alpha-\theta^g$. Then the lengthening along $\mathbf{Y}$ axis and the shortening along the $\mathbf{X}$ axis are actually the difference in length between the long diagonal $\overline{CD}$ and the short diagonal $\overline{AB}$, resulting in lengthening strain, given by $\varepsilon_h^g = (5-4\cos\alpha)^{1/2}-1$ and complementary shortening strain, $\varepsilon_w^g = -\varepsilon_h^g/(1+\varepsilon_h^g)$.

In the case of the basic Z-plasty [11–13], surgeons typically assume $\alpha = 60°$, and that the length of the incision is the same as that of the original cut. The simple geometric estimate predicts that the central limb rotates clockwise by 90° from $\mathbf{e}_y$ to $\mathbf{e}_x$, the height increases by 73%, and the width decreases by 42%. This also corresponds to the maximal possible rotation.

Such geometric estimates ignore the elastic response of skin [14], and raise the question of how these would effect the final state.

Here, we consider two related elastic models for the behavior of skin: the first a finely discretized mesh of linear springs (Fig. 1d) and the other represents the flaps and the incisions using coarse-grained springs (Fig.1e). In either case, we see that the final outcome is equivalent to introducing a disclination quadrupole of strength α at the wound site (Fig. 1f). We note that although a single disclination has unbounded deformation and divergent elastic energy, a disclination quadrupole has zero net disclination charge and restricts the deformation to a finite region [15]. Furthermore, the quadrupole is the lowest order disclination multipole that preserves the original tissue area, minimizes deformations in the far field, making Z-plasty surgery practical. However, in the case that we consider here, the elastic deformation around the quadruple involves both large rotation and large strain.

Our minimal spring model ignores the continuous deformation of the flaps and the surrounding regions and instead treats just the deformations of the vertices $\{A, B, C, D\}$, to their new locations $\{A', B', C', D'\}$, and the deformations of each side of the incisions which are treated as spring-like edges, with natural lengths corresponding to the lengths of the initial incisions. Because of the initial symmetry, we shall assume that $\overline{A'C'} = \overline{B'D'}$, $\overline{AA'} = \overline{BB'}$, $\overline{CC'} = \overline{DD'}$ and $\angle A'C'D' = \angle C'D'B'$. This results in the energy:

$$F = \kappa\left(\overline{AA'}\right)^2 + \kappa\left(\overline{CC'}\right)^2 + \kappa\left(\overline{C'D'}-1\right)^2 + \kappa\left(\overline{A'C'}-1\right)^2 + \kappa\left(\overline{A'D'}-2\sin(\tfrac{\alpha}{2})\right)^2, \qquad (1)$$

where all lengths have been rescaled by $\ell = 1$, such that $l_3 = 2\sin(\alpha/2)$, and where we have assumed that all springs have an identical elastic constant κ. Setting the values of $A' = \{x_a, y_a\}$ and $C' = \{x_c, y_c\}$, we can numerically minimize the elastic energy for different value of α to find a rough estimate of the geometry of the incisions post Z-plasty.

We also use a more refined model where we replace the skin with a discretized equilateral triangular mesh of

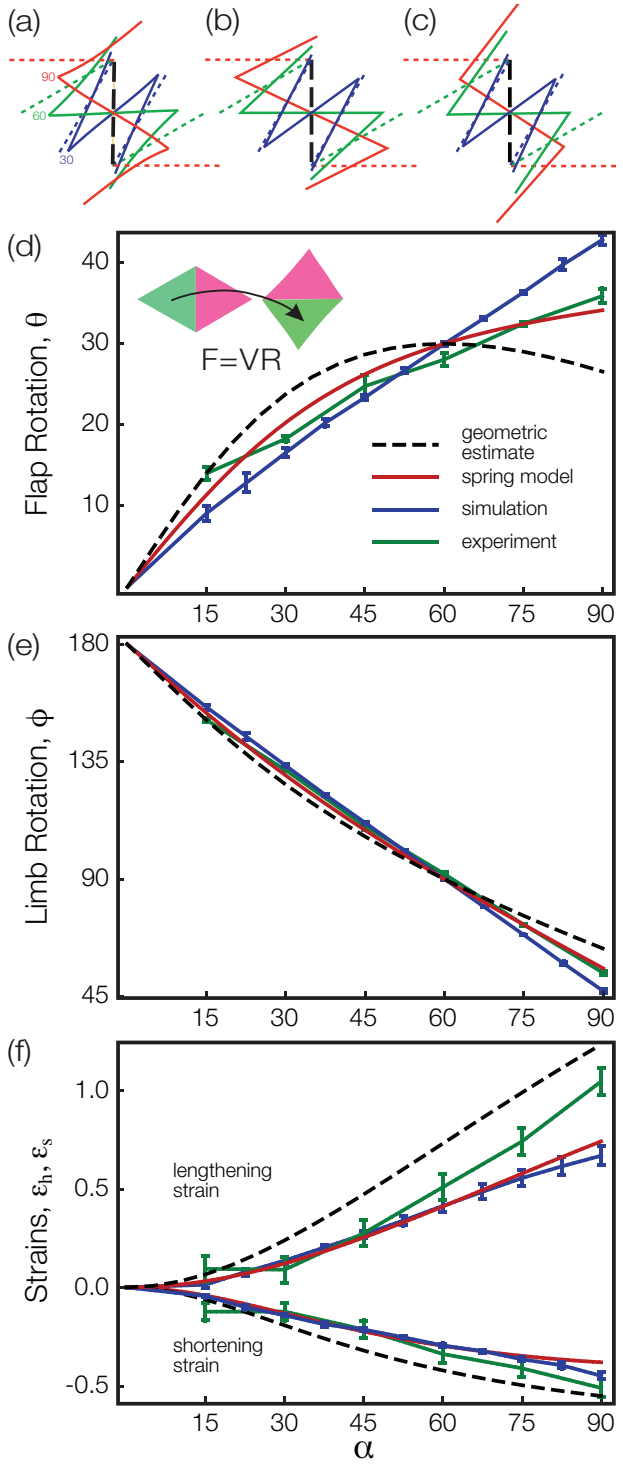

FIG. 2. a-c) Initial (dotted lines) and final (solid lines) geometries for different incision angles $\alpha = 30°, 60°, 90°$ for pre-strain 0.5 : 0.25. Results from the fine-grained simulation are shown in a), and those from the simple spring model in b), while in c), we show the results from a simple physical experiment using a sheet of foam rubber. The rotation angle of d) a flap, θ, e) the central limb, ϕ as a function of the incision angle α. f) Transverse lengthening ε_h and lateral shortening ε_w as a function of incision angle α.

freely-jointed linear elastic springs where the energies and lengths have been rescaled such that the spring constant and rest length are unity; this simple network yields results similar to those obtained using finite element simulations [17, 18], but is inexpensive. The spring network naturally accounts for geometric nonlinearities, and in principle could also account for material nonlinearities, but we ignore these here. We use a mesh of size 500×500, and first pre-stretch the sheet anisotropically with traction forces $\mathbf{f}_0$ applied at the boundary nodes so that $\epsilon_x^0 > \epsilon_y^0$. To mimic the process of Z-plasty surgery, we use the following protocol: (1) Cutting- The linear z-shaped incision is generated on the pre-stretched mesh by breaking springs along the incision. (2) Topological transposition- A geometric transformation $\mathbf{x} = \mathbf{F}_0\mathbf{X}$ is applied to the flaps so that $\Delta CAB \rightarrow \Delta CDB$ and $\Delta ABD \rightarrow \Delta ACD$ (shown in the inset of Fig. 2b), where $\mathbf{x}$ and $\mathbf{X}$ are the new and old positions of the flap, and $\mathbf{F}_0$ is the deformation gradient defined by the three vertices of a flap before and after transposition [16]. (3) Stitching and relaxation- The cut between the relocated limbs is "stitched" by adding new springs connecting opposing nodes, and the elastic energy of the spring network is minimized via a conjugate gradient method with constant traction $\mathbf{f}_0$ at the boundaries. As a result, the relocated flaps induces a strong local distortion and displays lengthening and shortening, as shown in Fig. 1b),d). We quantify the mechanical response for different tip angles $\alpha \in [15°, 90°]$, limb length $\ell = 100$, and different pre-strain $\varepsilon_x^0 : \varepsilon_y^0 = 0.4 : 0.2, 0.5 : 0.25, 0.6 : 0.2, 0.6 : 0.3, 0.6 : 0.4, 0.6 : 0.5$.

In Fig. 2a-c) we show the initial (dashed) and final (solid) geometries for three angles $\alpha = 30°, 60°, 90°$ subjected to the same pre-strain $\varepsilon_x^0 : \varepsilon_y^0 = 0.5 : 0.25$ determined from our numerical simulations (Fig. 2a), simple spring model (Fig. 2b) and physical experiment (Fig 2c). Four quantities serve as the basis for our comparison between the geometric (surgical) estimate and our two models: the rotation of each flap, θ (Fig. 2d), the rotation of the limb ϕ (Fig. 2e) and the strains, ε_h and ε_w (Fig. 2f).

The transformed geometries based on both our elastic models agree qualitatively with one another over the entire range of incision angles, but differ from the purely geometric model. In the purely geometric model, the flaps are not allowed to shear, and the final triangular flap is congruent to the initial one. Both spring models allow for the elastic deformation to be partially accommodated by a shearing transformation, which accounts for the qualitative difference that we see. Most interestingly, our physical experiment and all three models predict the same limb rotation angle of 90° for just one value of the incision, $\alpha = 60°$, and thus potentially minimize tearing stress on an anisotropically loaded wound. This result is a physical justification for the basic $\alpha = 60°$

Z-plasty, as it is the only value where the geometric and elastic models coincide. In Fig. 2f), we show the lengthening strains perpendicular to the original cut ϵ_h and shortening strain parallel to it ϵ_w, and again see that while the elastic models are in agreement, the geometric estimate overestimates the post-plasty strain; the source of this discrepancy lies in the strong local nonlinearity of the deformation field near the disclinations. We note that the only deviation between the models and experiment occurs in the lengthening strain ε_h for very large α, which corresponds to the strongly non-linear regime. This typically necessitates out-of-plane buckling and is, therefore, not frequently used by surgeons.

Having evaluated the geometric consequences of an elastic model for the Z-plasty, we now evaluate the tension-relief effects of Z-plasty on the main wound and the auxiliary incisions. This is most naturally described in terms of the stresses associated with tearing open the cuts: σ_{11}, shearing along the cuts: σ_{12}, and stretching the cuts: σ_{22} (Fig. 3a) for a particular choice of $\alpha = 60°$. Fig. 3b shows the average stress along the cut C, defined by $\bar{\sigma}_{\alpha\beta} = \int_C \widetilde{\sigma}_{\alpha\beta} ds / \int_C ds$ rescaled by the horizontal pre-stress σ_x^0, for $15° \leq \alpha \leq 90°$. We note that the average stretching stress, $\overline{\sigma}_{22}$, increases monotonically with α. Noting the small change in the lengths of the side limbs, the main contribution to $\overline{\sigma}_{22}$ comes from the geometric lengthening of the central limb that scales with $\varepsilon_h^g = (5 - 4\cos\alpha)^{1/2}$. The shear stress $\bar{\sigma}_{12}$ is relatively small, and does not vary much with α.

The energy density associated with the surgery contains four nearly singular regions, as expected from a disclination quadrupole (Fig. 3c). This can be estimated as the result of superposition of uniform deformation from the pre-strain and the localized deformation of the defect. For a positive disclination, a wedge of material is removed, leaving the remaining tissue under tension, whereas in a negative disclination, the addition of a wedge of material compresses the surrounding tissue. This results in two energetic maxima, at C' and D', and two minima, at A' and B', shown in Fig. 3c, corresponding to the mesh in Fig. 1d.

Our study of a classical plastic surgery technique, the Z-plasty – a topological rearrangement of skin in the neighborhood of a cut, combines simple elastic notions to complement previous geometrical approaches. Our two spring-based elastic models compare well with physical experiments but coincide with the geometric *ansatz* used by surgeons only for $\alpha = 60°$, when limb rotation is maximized, allowing the primary wound to rotate by 90°. For other values of α our model enables sets the stage for a consideration of stress fields and elastic deformations that surgeons can optimize when considering the initial choice of incision to increase efficacy of post-surgical outcomes.

We conclude with a few perspectives. From a topological point of view, several other plasty operations,

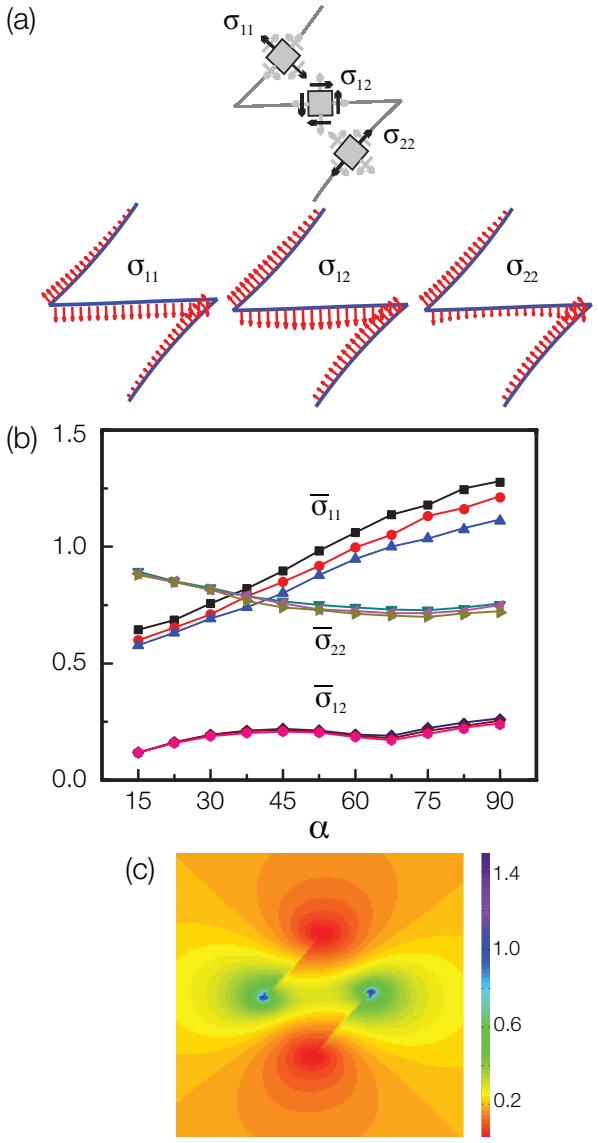

FIG. 3. The stress and elastic energy obtained from our refined simulation. a) The definition of pulling stress σ_{11}, shearing stress σ_{12}, and stretching stress σ_{22} along the incision. b) The averaged stress line integrals of $\overline{\sigma}_{11}$, $\overline{\sigma}_{12}$, and $\overline{\sigma}_{22}$ as function of tip angle α. c) The elastic energy field with pre-strain 50 : 25 and tip angle 60°. The scaled elastic energy density in the far field is 0.23.

such as Y-plasty, which converts a "V" shaped incision into a "Y" shape, or W-plasty, wherein multiple Z-plasties are conducted along a long primary wound, can be considered as multipole expansions of disclinations. From a physical perspective, Z plasty is a combination of kirigami, where cuts are determined for the purpose of creating distinct three-dimensional geometries [19, 20] and elasticity, since the goal is to perform planar topological manipulations while keeping the final skin topography as close as possible to that of the underlying tissue. This would not be possible were it not for the

intrinsic elasticity of the dermis. In practice, surgeons find dog-ears (raised conical deformations of the skin) at A' and B' if the environmental stretching is not strong enough to compensate the disclination-induced compression. From a biological/medical perspective, our study is just the beginning as we need to also account for factors associated with wound healing dynamics that are themselves affected by the local strain state in the vicinity of the cut.

We thank Amit Patel for contributing to the project in its preliminary stages, and the National Natural Science Foundation of China (11272303), the Wyss Institute and the MacArthur Institute for partial financial support.

[1] M. A. Hardy, Phys. Ther. **69**, 1014 (1989).
[2] S. Aarabi, FASEB J **21**, 3250 (2007).
[3] F. J. Grinnell, Cell Biol. **124**, 401 (1994).
[4] T. L. Tuan & L. S. Nichter, Mol. Med. Today **4**, 19 (1998).
[5] S. D. Zimmerman, Am. J. Physiol. Heart Circ. Physiol. **278**, 194 (2000).
[6] E. Cerda, J. Biomech **38**, 1598 (2005).
[7] W. E. Horner, Am. J. Med. Sci. **21**, 105 (1873).
[8] A. F. Borges, Br. J. Plastic Surgery **26**, 237 (1973).
[9] A. Prez-Bustillo, B. Gonzlez-Sixto, & M. A. Rodrguez-Prieto, Actas Dermo-Sifiliogrficas (English Edition), **104** 17 (2013).
[10] Here we keep the lengths of the side limbs equal to the central wound, as it would otherwise lead to the effective insertion of dislocations and discontinuities in the traction along the stitched cuts.
[11] I. A. McGregor, British J. Plastic Surgery **9**, 256 (1957).
[12] S. Ellur. *Indian J Plast Surg*, **41** 99 (2008).
[13] S. Ellur & N. Guido. *Indian J Plast Surg*, **42** 82 (2009).
[14] D. W. Furnas & G. W. Fischer, British J. Plast. Surg. **24**, 144 (1971).
[15] A. E. Romanov, Eur. J. Mech. A-Solid **22**, 77 (2003).
[16] T. Belytschko, W. L. Liu, & B. Moran, *Nonlinear Finite Elements for Continua and Structures* (John Wiley and Sons Ltd., 2000.
[17] E. Sifakis, J. Hellrung, J. Teran, A. Oliker & C. Cutting, https://www.math.ucla.edu/ jteran/papers/SHTOC09.pdf (2009).
[18] E. Kitta & M. Akimoto, *J. Nippon Med. Sch.* **80** 218 (2013).
[19] T. Castle, *et al*, Phys. Rev. Lett. **113**, 245502 (2014).
[20] D. M. Sussman, *et al*, Proc. Nat. Acad. Sci. **112**, 7449 (2015).